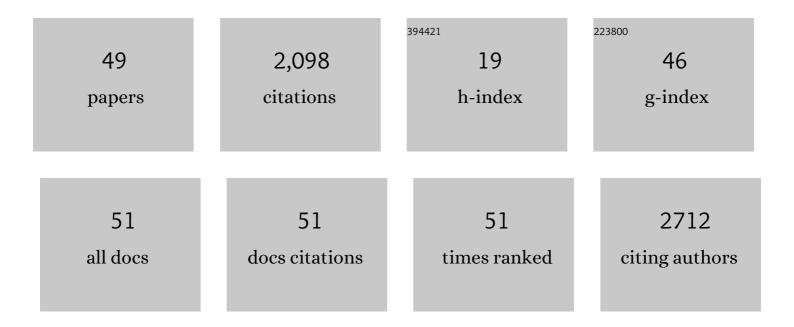
Yong Chan Choi

List of Publications by Year in descending order

Source: https://exaly.com/author-pdf/8027823/publications.pdf Version: 2024-02-01



#	Article	IF	CITATIONS
1	Highly Improved Sb ₂ S ₃ Sensitizedâ€Inorganic–Organic Heterojunction Solar Cells and Quantification of Traps by Deepâ€Level Transient Spectroscopy. Advanced Functional Materials, 2014, 24, 3587-3592.	14.9	454
2	Nanostructured TiO2/CH3NH3PbI3 heterojunction solar cells employing spiro-OMeTAD/Co-complex as hole-transporting material. Journal of Materials Chemistry A, 2013, 1, 11842.	10.3	301
3	Sb ₂ Se ₃ ‣ensitized Inorganic–Organic Heterojunction Solar Cells Fabricated Using a Single‣ource Precursor. Angewandte Chemie - International Edition, 2014, 53, 1329-1333.	13.8	145
4	Efficient Sb ₂ S ₃ ‣ensitized Solar Cells Via Single‣tep Deposition of Sb ₂ S ₃ Using S/Sbâ€Ratioâ€Controlled SbCl ₃ â€Thiourea Complex Solution. Advanced Functional Materials, 2015, 25, 2892-2898.	14.9	145
5	Efficient Inorganicâ€Organic Heterojunction Solar Cells Employing Sb ₂ (S _{<i>x</i>} /Se _{1â€<i>x</i>}) ₃ Gradedâ€Composition Sensitizers. Advanced Energy Materials, 2014, 4, 1301680.	19.5	123
6	Ferroelectricity in Highly Ordered Arrays of Ultra-Thin-Walled Pb(Zr,Ti)O ₃ Nanotubes Composed of Nanometer-Sized Perovskite Crystallites. Nano Letters, 2008, 8, 1813-1818.	9.1	112
7	Efficient Nanostructured TiO ₂ /SnS Heterojunction Solar Cells. Advanced Energy Materials, 2019, 9, 1901343.	19.5	86
8	Efficient room temperature aqueous Sb ₂ S ₃ synthesis for inorganic–organic sensitized solar cells with 5.1% efficiencies. Chemical Communications, 2015, 51, 8640-8643.	4.1	78
9	Efficient Solar Cells Based on Lightâ€Harvesting Antimony Sulfoiodide. Advanced Energy Materials, 2018, 8, 1701901.	19.5	76
10	CuSbS ₂ ‣ensitized Inorganic–Organic Heterojunction Solar Cells Fabricated Using a Metal–Thiourea Complex Solution. Angewandte Chemie - International Edition, 2015, 54, 4005-4009.	13.8	72
11	Direct observation of alumina nanowire formation from porous anodic alumina membrane via the droplet etching method. Nanotechnology, 2006, 17, 355-359.	2.6	52
12	Controlled growth of SbSI thin films from amorphous Sb2S3 for low-temperature solution processed chalcohalide solar cells. APL Materials, 2018, 6, .	5.1	29
13	Tribological effects of pores on an anodized Al alloy surface as lubricant reservoir. Current Applied Physics, 2011, 11, S182-S186.	2.4	28
14	Effects of a perfluorinated compound as an additive on the power conversion efficiencies of polymer solar cells. Solar Energy Materials and Solar Cells, 2011, 95, 1908-1914.	6.2	26
15	Antisolvent-assisted powder engineering for controlled growth of hybrid CH3NH3PbI3 perovskite thin films. APL Materials, 2017, 5, .	5.1	25
16	Systematic control of nanostructured interfaces of planar Sb 2 S 3 solar cells by simple spin-coating process and its effect on photovoltaic properties. Journal of Industrial and Engineering Chemistry, 2017, 56, 196-202.	5.8	24
17	Recent Progress in Fabrication of Antimony/Bismuth Chalcohalides for Lead-Free Solar Cell Applications. Nanomaterials, 2020, 10, 2284.	4.1	22
18	Controlled Growth of BiSI Nanorod-Based Films through a Two-Step Solution Process for Solar Cell Applications. Nanomaterials, 2019, 9, 1650.	4.1	21

Yong Chan Choi

#	Article	IF	CITATIONS
19	Structure of alumina nanowires synthesized by chemical etching of anodic alumina membrane. Physica E: Low-Dimensional Systems and Nanostructures, 2007, 36, 140-146.	2.7	19
20	Enhanced performance of perovskite solar cells by incorporation of a triphenylamine derivative into hole-transporting poly(3-hexylthiophene) layers. Journal of Industrial and Engineering Chemistry, 2019, 73, 175-181.	5.8	19
21	Template-directed formation of functional complex metal-oxide nanostructures by combination of sol–gel processing and spin coating. Materials Science and Engineering B: Solid-State Materials for Advanced Technology, 2006, 133, 245-249.	3.5	17
22	Controlled growth of organic–inorganic hybrid CH ₃ NH ₃ PbI ₃ perovskite thin films from phase-controlled crystalline powders. RSC Advances, 2016, 6, 104359-104365.	3.6	16
23	Compositional Engineering of Antimony Chalcoiodides via a Two-Step Solution Process for Solar Cell Applications. ACS Applied Energy Materials, 2022, 5, 5348-5355.	5.1	13
24	Morphology Transformation of Chalcogenide Nanoparticles Triggered by Cation Exchange Reactions. Chemistry of Materials, 2019, 31, 268-276.	6.7	12
25	Enhanced Power Conversion Efficiency of Dye-Sensitized Solar Cells by Band Edge Shift of TiO2 Photoanode. Molecules, 2020, 25, 1502.	3.8	11
26	One-Step Solution Deposition of Antimony Selenoiodide Films via Precursor Engineering for Lead-Free Solar Cell Applications. Nanomaterials, 2021, 11, 3206.	4.1	11
27	?Correlation between Self-Organized Pore Formation Behaviors and Current-Time Characteristics in Porous Anodic Alumina: Quantitative Analysis of Voltage Dependence of Pore Morphological Changes. Journal of the Korean Physical Society, 2010, 56, 113-119.	0.7	10
28	Effects of a TiO 2 :CaO barrier layer on the back electron transfer in TiO 2 -based solar cells. Journal of Industrial and Engineering Chemistry, 2017, 50, 96-101.	5.8	10
29	Synthesis of Metal-oxide Nanotubes by Using Template-directed Growth in Conjunction with the Sol-gel Process and a Spin-coating Technique. Journal of the Korean Physical Society, 2011, 59, 2551-2555.	0.7	7
30	Nanopore Domain Growth Behavior by Nanopore Changes Near Domain Boundaries in Porous Anodic Alumina. Journal of Nanoscience and Nanotechnology, 2011, 11, 1346-1349.	0.9	6
31	Lubricating layer formed on porous anodic alumina template due to pore effect at water lubricated sliding and its properties. Thin Solid Films, 2012, 521, 3-6.	1.8	6
32	Strong pore-size dependence of the optical properties in porous alumina membranes. Journal of the Korean Physical Society, 2013, 63, 1789-1793.	0.7	6
33	Effects of Wall Thickness on Morphology and Structure of Lead Titanate Nanotubes. Ferroelectrics, 2013, 454, 29-34.	0.6	5
34	Molecular Weight Effects of Biscarbazole-Based Hole Transport Polymers on the Performance of Solid-State Dye-Sensitized Solar Cells. Nanomaterials, 2020, 10, 2516.	4.1	5
35	Effects of Thermal Treatment Conditions on the Phase Formation and the Morphological Changes of Sol-gel Derived 0.67Pb(Mg1/3Nb2/3)O3-0.33PbTiO3 Thin Films. Journal of the Korean Physical Society, 2011, 58, 668-673.	0.7	5
36	Synthesis and Characterization of Lead Zirconate Titanate Nanotubes. Ferroelectrics, 2007, 356, 236-241.	0.6	3

Yong Chan Choi

#	Article	IF	CITATIONS
37	Paramagnetism in Pb(Zr,Ti)O3 nanotube arrays at low temperatures. Journal of the Korean Physical Society, 2012, 60, 1097-1101.	0.7	3
38	Effects of etching time on the bottom surface morphology of ultrathin porous alumina membranes for use as masks. Journal of the Korean Physical Society, 2012, 61, 1660-1665.	0.7	3
39	Photoluminescence of ultra-thin-walled Pb(Zr,Ti)O3 nanotubes synthesized in the porous alumina membrane template-directed method. Journal of the Korean Physical Society, 2013, 63, 1040-1044.	0.7	3
40	Synthesis of Crystalline Lead Di-Oxide Nanowires and Their Electron-Beam-Induced Phase Transformation to Oxygen Deficient Lead Mono-Oxide. Journal of the Korean Physical Society, 2007, 51, 2045.	0.7	3
41	Photovoltaic Performance of Dye-Sensitized Solar Cells with a Solid-State Redox Mediator Based on an Ionic Liquid and Hole-Transporting Triphenylamine Compound. Energies, 2022, 15, 2765.	3.1	3
42	Surface-adsorbate-induced fluorescence-type Raman background of Pb(Zr0.4Ti0.6)O3 nanotubes. Current Applied Physics, 2012, 12, 1272-1277.	2.4	2
43	Effects of Sintering Temperature on the Pyrochlore Phase in PZT Nanotubes and Their Transformation to the Perovskite Phase by Coating with PbO Multilayers. Journal of Nanoscience and Nanotechnology, 2014, 14, 8554-8560.	0.9	2
44	Effects of pyrolysis temperature on structural, Raman, and infrared properties of perovskite PbTiO3 nanotubes. Journal of the Korean Physical Society, 2016, 68, 545-550.	0.7	2
45	Key Factors Affecting the Performance of Sb ₂ S ₃ -sensitized Solar Cells During an Sb ₂ S ₃ Deposition via SbCl ₃ -thiourea Complex Solution-processing. Journal of Visualized Experiments,	0.3	2
46	ZUT8, , Lead Zirconate Titanate Nanowire Growth Via Spin Coating in Conjunction with Sol-Gel Process. Ferroelectrics, 2007, 356, 230-235.	0.6	1
47	Self-assembled growth of nanocomposites consisting of TiO2nanopillars and Pb(Zr0.52Ti0.48)O3thin films. Nanotechnology, 2009, 20, 425601.	2.6	1
48	THE DEPENDENCE OF ALUMINA NANOWIRE FORMATION FROM POROUS ANODIC ALUMINA MEMBRANES ON THE ETCHING SOLUTION. Modern Physics Letters B, 2012, 26, 1150017.	1.9	1
49	Effects of Anodization Time and Temperature on the Pore Arrangement of Porous Anodic Alumina Anodized in Sulfuric Acid. New Physics: Sae Mulli, 2013, 63, 1249-1253.	0.1	1